

TUM

INSTITUT FÜR INFORMATIK

Prediction of Mechanical Lung Parameters Using Gaussian Process Models

Steven Ganzert, Stefan Kramer, Knut Möller,
Daniel Steinmann, Josef Guttmann



TUM-I0911

April 09

TECHNISCHE UNIVERSITÄT MÜNCHEN

TUM-INFO-04-I0911-100/1.-FI
Alle Rechte vorbehalten
Nachdruck auch auszugsweise verboten

©2009

Druck: Institut für Informatik der
 Technischen Universität München

Prediction of Mechanical Lung Parameters Using Gaussian Process Models

Steven Ganzert^{1*}, Stefan Kramer², Knut Möller³, Daniel Steinmann¹, and
Josef Guttman¹

¹ University Hospital Freiburg, Department of Experimental Anesthesiology,
D-79106 Freiburg, Germany

² Technische Universität München, Institut für Informatik / I12,
D-85748 Garching b. München, Germany

³ Furtwangen University, Department of Biomedical Engineering,
D-78054 Villingen-Schwenningen, Germany

Abstract. Mechanical ventilation can cause severe lung damage by inadequate adjustment of the ventilator. We introduce a Machine Learning approach to predict the pressure-dependent, non-linear lung compliance, a crucial parameter to estimate lung protective ventilation settings. Features were extracted by fitting a generally accepted lumped parameter model to time series data obtained from ARDS (adult respiratory distress syndrome) patients. Numerical prediction was performed by use of Gaussian processes, a probabilistic, non-parametric modeling approach for non-linear functions.

1 Medical Background and Clinical Purpose

Under the condition of mechanical ventilation a high volume distensibility – or *compliance* C – of the lung is assumed to reduce the mechanical stress to the lung tissue and hence irreversible damage to the respiratory system. A common technique to determine the *maximal compliance* C_{max} inflates the lung with almost zero flow (so-called ‘static’ conditions) over a large PV range (inspiratory capacity). The inspiratory limb of the corresponding PV curve typically shows a sigmoid shape. As C is determined by the change of respiratory volume V divided by the change of applied respiratory pressure P , i.e. $C = \Delta V / \Delta P$, C_{max} is found at the curve interval with the steepest slope. This is supposed to be the optimal PV range for lung protective ventilation [1] (see Fig. 1). Within Super-syringe maneuvers [1] rapid flow interruptions are iteratively performed after consecutive, equally sized volume inflations. These flow interruptions reveal characteristic stress relaxation curves, exponentially approximating the plateau pressure level P_{plat} (see Fig. 2, insert). The spring-and-dashpot model [2] is assumed to represent the viscoelastic behavior of the lung tissue. Fitting this model to flow interruption data provides the four parameters C , *respiratory resistance* R , *viscoelastic compliance* C_{ve} and *resistance* R_{ve} which are non-linearly related

* Corresponding author, e-mail: steven.ganzert@uniklinik-freiburg.de

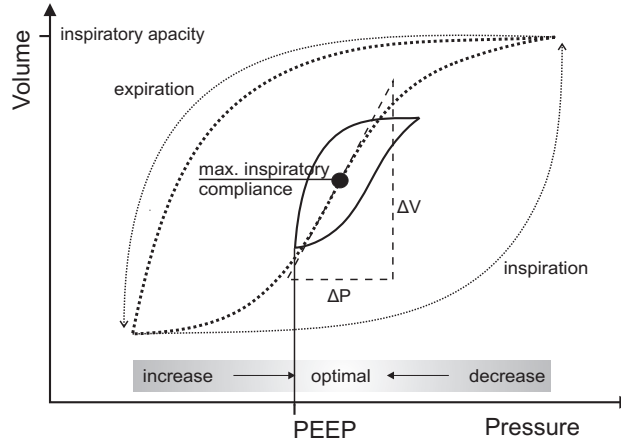


Fig. 1. Schematized PV loops measured under static (dotted large loop: inspiratory flow ≈ 0 ml/sec) and dynamic (straight small loop: inspiratory flow $\gg 0$ ml/sec) conditions. The static loop covers the range of the inspiratory capacity. Within the inspiratory limb the maximum compliance is detected at the interval with the steepest slope. For the dynamic loop, the PEEP (positive end-expiratory pressure) is adjusted to optimize, i.e. maximize compliance. The pressure gap between the static and the dynamic curve is effected by the flow induced pressure fraction under dynamic conditions.

to P_{plat} . In its entirety these parameters numerically reflect the mechanical status of the respiratory system. The purpose of this study is to model statistically the pressure-dependent non-linear behavior of the compliance. The individualized prediction of this mechanical lung parameter could assist the physician when individually adjusting the applied pressure level in order to reduce the risk of ventilator induced lung injury.

2 Gaussian Processes and Modeling Task

Non-linear regression problems are generally modeled by parametrizing a function $f(x)$ with parameters w to $f(x;w)$. Gaussian Processes (GPs) [3–5] introduce a probabilistic approach to this field: the parametrized function can be rewritten as a linear combination of non-linear basis functions $\phi_h(x)$, i.e. $f(x;w) = \sum_{h=1}^H \omega_h \phi_h(x)$. Under the assumption that the distribution of w is Gaussian with zero mean, the linear combination of the parametrized basis functions produces a result which is distributed Gaussian as well. Assuming that the target values differ by additive Gaussian noise from the function values, the prior probability of the target values is also Gaussian. The linear combination of parametrized basis functions can be replaced by the covariance matrix of the function values and inference from a new feature observation is done by evaluation of this matrix. The precision of these predictions essentially depends on the covariance- or kernel-function, which evaluates the degree of covariance between

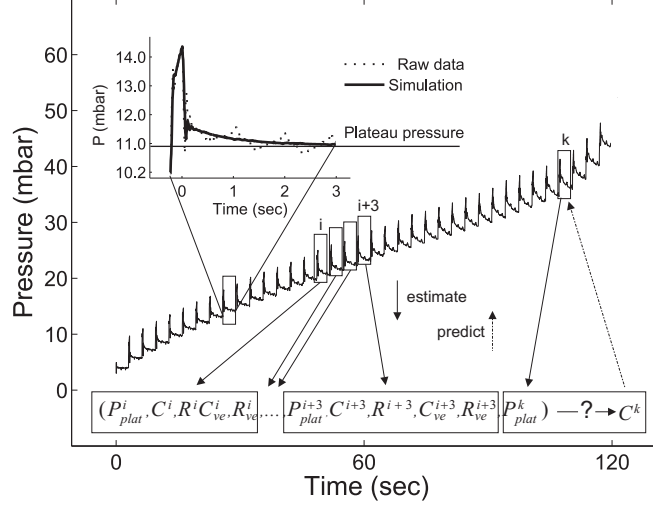


Fig. 2. Sample pressure time series for Super-syringe maneuver. For all occlusion steps the attribute values C , R , C_{ve} and R_{ve} were estimated by a model fit. Based on the estimated values of 4 consecutive occlusion steps i to $i + 3$ the compliance C was predicted for the plateau pressure at step k . Inset: Pressure raw data and simulation for one sample volume step with following airway occlusion. At the end of the occlusion the plateau pressure was approximated. Simulation was performed by inserting the estimated parameters into the lumped parameter model and application of the corresponding flow time series. The oscillations in the raw data curve are of cardiogenic origin and are not represented in the model.

the target values. A prior assumption on our modeling task is that the hypothesis space consists of the derivatives of sigmoid-like shaped functions ($C = \Delta V / \Delta P$) (see Fig. 1). As all measured patient data sets imply general as well as individual characteristics of the ARDS lung, the shape of these functions ought to be distributed according to a prior probability. Therefore, we hypothesized that our modeling task would benefit from the probabilistic modeling of (possibly) non-linear functions as provided by GP modeling. In the present study inferences were made from the status of the respiratory system at a distinct plateau pressure range to the compliance value at a different pressure level:

- (i) Prediction of the compliance-pressure curve covering the range of the inspiratory capacity.
- (ii) Prediction of the maximum compliance value C_{max} and its corresponding plateau pressure value $P_{plat}(C_{max})$.
- (iii) Prediction, if the pressure level should be increased, decreased or retained in order to achieve C_{max} (which we refer to as *trend* in the following).

3 Materials and Methods

3.1 Raw Data

The data for this retrospective study were obtained from a multicenter study including patients mechanically ventilated due to severe ARDS [6, 7]. Automated Super-syringe maneuvers [8] were performed completely for 20 patients. During a single maneuver, the ventilatory system repetitively applied volume steps of 100 ml with constant inspiratory airflow rates (558 ± 93 mL/sec) up to a maximum plateau pressure of 45 mbar. At the end of each volume step, airflow was interrupted for 3 seconds (see Fig. 2). The maneuvers consisted of 5 to 39 occlusions, depending on the status of the individual lung. Flow and pressure data were measured proximally to the endotracheal tube at a sample rate of 125 Hz. The pressure drop at the endotracheal tube ΔP_{ETT} was calculated by the Rohrer equation $\Delta P_{ETT} = K_1 \times \dot{V} + K_2 \times \dot{V}^2$ and subtracted from the measured airway pressure, with Rohrer-coefficients K_1 and K_2 according to [9]. As for two patients the tube-types were not recorded and thus the tracheal pressure could not be calculated, 18 patients were included.

3.2 Feature Extraction and Preprocessing

For each flow interruption step k , the attributes C^k , R^k , C_{ve}^k and R_{ve}^k were estimated by fitting the electrical analog of a spring-and-dashpot model [10] to the data (see Fig. 3). P_{plat}^k was approximated by the mean pressure of the last 0.5 sec of flow interruption (see Fig. 2 insert). The pressure data of each step was corrected by the P_{plat} -offset of the preceding step. The initial system status was represented by the fitted parameter and measured plateau pressure values of 4 consecutive steps i to $i + 3$. For all possible states that can be determined by such quadripartite steps the compliance was predicted as target value C^k for all plateau pressure levels P_{plat}^k . Therefore the feature samples consisted of the 22-tupel $(P_{plat}^{i...i+3}, C^{i...i+3}, R^{i...i+3}, C_{ve}^{i...i+3}, R_{ve}^{i...i+3}, P_{plat}^k, C^k)$ (see Fig. 2).

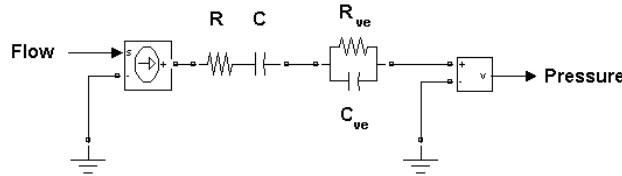


Fig. 3. Electrical analog of a spring-and-dashpot model. R and C denote the Newtonian component, R_{ve} and C_{ve} the viscoelastic component of the model. The input signal was determined by the measured respiratory flow, the output signal by the measured respiratory pressure data.

3.3 Data Modeling and Experimental Setting

For Gaussian Process Modeling a Pearson VII function-based universal kernel [11] with $\sigma = 1$, $\omega = 1$ and a noise-level of 1 was applied. As reference method for prediction task (i) the M5P [12] algorithm was evaluated. M5P generates a combination of conventional decision trees with linear regression functions as model trees. For task (ii) and (iii) the measured and the predicted C_{max} values were calculated by fitting a degree 3 polynom to the raw data and to the modeled compliance-pressure curve respectively. Then the extreme values of the polynom were calculated. If no local maximum was located within the pressure-range [$\min(P_{plat}^1, \dots, P_{plat}^n), \max(P_{plat}^1, \dots, P_{plat}^n)$] covered by the individual Super-syringe maneuver, C_{max} was set to the C value at the minimum or maximum pressure value, depending on the slope of the curve. For task (iii) it was determined, if each the measured and the predicted $P_{plat}(C_{max})$ was estimated within the initial pressure range [$P_{plat}^i, P_{plat}^{i+3}$], or if it was higher or lower. Accordingly the *trends* for measured and modeled data were evaluated and compared. All algorithms for parameter prediction were applied as implemented in the data mining software WEKA [13]. Two experimental settings were evaluated:

1. Separately for each single patient data set (i.e. Super-syringe measuring) the three prediction tasks were performed. This experimental setting should confirm the suitability of GP models for the given data.
2. To investigate the practical applicability of the approach, training and test set were repetitively built for each patient data set. For each run, the training set consisted of all patient-data sets except one, which was used as test set.

3.4 Performance Measures

For prediction task (i), the performance was measured by the correlation coefficient (CC) of the model prediction. Other performance measures like error estimations were supposed to be inadequate as the raw data showed high variability. For task (ii) the percentage difference between the maximum compliance (respectively its corresponding P_{plat}) determined from the raw data and the predicted maximum compliance (respectively P_{plat}) was calculated. Task (iii) was evaluated by the percentage of correct predictions of the *trend*. Results are given as *mean* \pm *sd*.

4 Results and Discussion

4.1 Experimental Setting (1)

(i) Prediction of the compliance curve by GP modeling reached an averaged CC of 0.78 ± 0.16 , the reference Method (M5P) an averaged CC of 0.92 ± 0.23 . (ii) While the predicted maximum compliance C_{max} averagely differed with $9.7 \pm 6.5\%$ from C_{max} estimated from the raw data, $P_{plat}(C_{max})$ differed with an average of $5.4 \pm 10.6\%$. (iii) The prediction, if the pressure level should be increased, decreased or retained was correctly answered in $93.2 \pm 11.1\%$ (see Table 2).

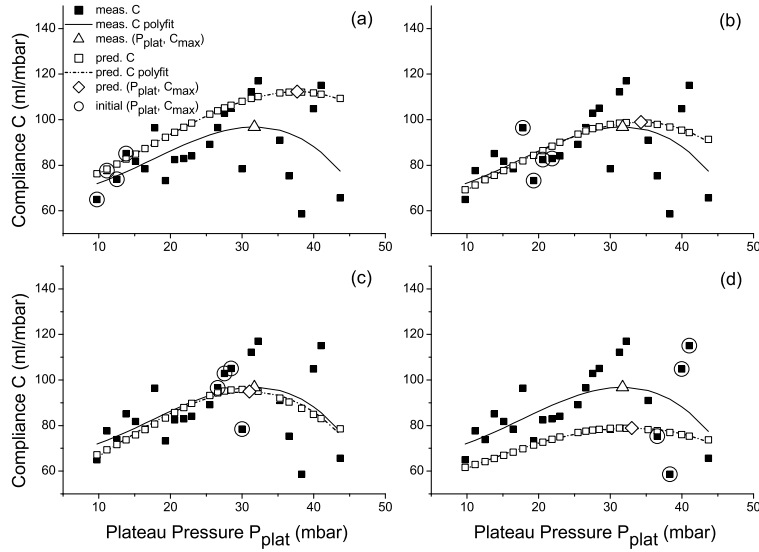


Fig. 4. Sample results for one patient in experimental setting (2). Predictions of C ($pred. C$) are based on the respiratory status at low (a), intermediate (b), (c) and high (d) levels of P_{plat} ($initial (P_{plat}, C_{max})$). The variability of the measured (i.e., fitted) C values ($meas. C$) is clearly exhibited. Measured and predicted C_{max} and the corresponding P_{plat} ($meas. (P_{plat}, C_{max}), pred. (P_{plat}, C_{max})$) are determined by polynomial fits ($meas. C polyfit, pred. C polyfit$). Referring to the sigmoid-like shape of an inspiratory pressure-volume curve, the modeled curves approximate the 1st derivative of a sigmoid function.

4.2 Experimental Setting (2)

(i) The CC of the learned model had an average of 0.34 ± 0.24 for GP modeling and 0.18 ± 0.22 for the M5P algorithm. (ii) Predicted C_{max} differed with an average of $34.3 \pm 34.3\%$ and predicted $P_{plat}(C_{max})$ with $40.7 \pm 70.1\%$ from the maximum compliance and corresponding pressure values derived from the raw data. (iii) Prediction of the trend for the pressure correction was in 2/3 of the cases ($66.3 \pm 30.3\%$) correct (see Table 3).

Performance within experimental setting (1) confirmed that GP modeling is basically suitable for the present task and problem representation. As hypothesized, the compliance-pressure curves were adequately modeled, having slopes of the first derivative of a sigmoid-like function (see Fig. 4). Differentiated characteristics for the individual patient datasets were expressed in differing curve slopes. Comparing the results of GP modeling and M5P for prediction task (i) within settings (1) and (2) leads to the assumption, that the M5P tends more to overfitting than GP modeling. This was perhaps down to the fact that for

the present problem the modeling of functions might provide a higher degree of abstraction and reduce the impact of noise. Nevertheless, individual compliance curves for new observations according to setting (2) showed rather poor results. While the prediction of C_{max} and $P_{plat}(C_{max})$ (task ii) as well as the prediction of the correct *trend* for the pressure correction (task iii) showed failure rates below 10% in setting (1), which might be sufficiently precise for an indication in medical practice, the results again were impaired within setting (2). Predictions with divergences of more than 30% for C_{max} and $P_{plat}(C_{max})$ and failure rates in a similar range for trend prediction provide at most a rough estimates. This implies that learning an individualized model might require an individualized feature selection.

5 Conclusions

To the best of our knowledge, this is the first time that mechanical lung parameters have been predicted by a statistical modeling approach. The results indicate that the combination of classical model fitting and statistical modeling is generally capable of solving this task. Nevertheless an individualized feature selection as pre-processing step should be brought into focus in future efforts.

References

1. Matamis, D., Lemaire, F., Harf, A., Brun-Buisson, C., Ansquer, J.C., Atlan, G.: Total respiratory pressure-volume curves in the adult respiratory distress syndrome. *Chest* **86** (1984) 58–66
2. Bates, J.H.T., Brown, K.A., Kochi, T.: Identifying a model of respiratory mechanics using the interrupter technique. In: Proceedings of the Ninth American Conference I.E.E.E. Engineering Medical Biology Society. (1987) 1802–1803
3. Krige, D.G.: A statistical approach to some basic mine valuation problems on the witwatersrand. *J. of the Chem., Metal. and Mining Soc. of South Africa* **52** (1951) 119–139
4. Mackay, D.J.C.: Introduction to gaussian processes. Technical report. Cambridge University (1999)
5. Rasmussen, C.E., Williams, C.K.I.: Gaussian Processes for Machine Learning. MIT Press, MA (2006)
6. Stahl, C.A., Möller, K., Schumann, S., Kuhlen, R., Sydow, M., Putensen, C., Guttman, J.: Dynamic versus static respiratory mechanics in acute lung injury and acute respiratory distress syndrome. *Crit. Care Med.* **34** (2006) 2090–8
7. Ganzert, S., Guttman, J., Kersting, K., Kuhlen, R., Putensen, C., Sydow, M., Kramer, S.: Analysis of respiratory pressure-volume curves in intensive care medicine using inductive machine learning. *Artif. Intell. Med.* **26** (2002) 69–86
8. Sydow, M., Burchardi, H., Zinserling, J., Ische, H., Crozier, T.A., Weyland, W.: Improved determination of static compliance by automated single volume steps in ventilated patients. *Intensive Care Med.* **17** (1991) 108–14
9. Guttman, J., Eberhard, L., Fabry, B., Bertschmann, W., Wolff, G.: Continuous calculation of intratracheal pressure in tracheally intubated patients. *Anesthesiology* **79** (1993) 503–513

10. Jonson, B., Beydon, L., Brauer, K., Mansson, C., Valind, S., Grytzell, H.: Mechanics of respiratory system in healthy anesthetized humans with emphasis on viscoelastic properties. *J. Appl. Physiol.* **75** (1993) 132–40
11. Üstün, B., Melssen, W.J., Buydens, L.M.C.: Facilitating the application of support vector regression by using a universal pearson vii function based kernel. *Chemometr. Intell. Lab.* **81** (2006) 29–40
12. Quinlan, J.R.: Learning with continuous classes. In: Proceedings of the Australian Joint Conference on Artificial Intelligence, World Scientific, Singapore (1992) 343–8
13. Witten, I.H., Frank, E.: *Data Mining: Practical machine learning tools and techniques*. 2 edn. Morgan Kaufmann, San Francisco (2005)

Tables

Table 1. Data: For setting (1) the pure test-sets, i.e. the extracted feature samples (22-tuples) of each single patient measurement (Super-syringe maneuver) were evaluated. For each run within setting (2) a training and test data set was built by excluding the data of a single patient which was used for testing. Besides the number of samples for training and testing for each patient, the maximum compliance values C_{max} with the corresponding plateau pressures $P_{plat}(C_{max})$ are given. The size of the data sets for each patient depended on the number of occlusions performed during the Super-syringe maneuver and thus by the number of extracted feature values.

<i>Patient</i>	<i>#Training</i>	<i>#Testing</i>	C_{max} mL/mbar	$P_{plat}(C_{max})$ mbar
1	4568	12	78.2	44.3
2	3500	1080	121.4	30.9
3	4322	270	74.2	30.3
4	4132	460	141.3	36.8
5	5034	18	28.0	36.7
6	4289	108	37.8	20.9
7	4498	572	96.8	31.1
8	5554	88	82.1	36.1
9	5180	550	81.4	23.9
10	5426	304	51.2	23.7
11	5460	270	153.1	29.9
12	5642	88	80.5	33.9
13	5352	378	62.2	20.1
14	5676	54	82.1	21.3
15	5726	4	40.3	11.0
16	5622	108	115.8	33.6
17	5622	108	120.0	32.6
18	5730	54	29.5	9.1

#Training, *#Testing*: number of samples for training and testing; C_{max} : Maximum compliance estimated from raw data; $P_{plat}(C_{max})$: Plateau pressure at which maximum compliance was estimated.

Table 2. Results for experimental setting (1): Prediction performed for each single patient (test) data set.

<i>Patient</i>	C_{max} ml/mbar mean±sd	$P_{plat}(C_{max})$ mbar mean±sd	<i>trend</i> %	ΔC_{max} %	$\Delta P_{plat}(C_{max})$ %	CC_{GP}	CC_{M5P}
1	62.8 ± 0.0	44.0 ± 0.00	100	19.6	0.0	0.99	0.98
2	141.6 ± 1.8	44.8 ± 0.53	67	16.6	45.1	0.59	0.99
3	72.4 ± 0.5	29.2 ± 0.04	100	2.4	3.7	0.83	0.98
4	131.0 ± 1.5	34.0 ± 0.35	100	7.3	7.5	0.85	0.98
5	25.9 ± 0.0	36.7 ± 0.00	100	7.6	0.0	0.91	0.94
6	34.3 ± 0.0	19.7 ± 0.01	100	9.3	5.9	0.89	0.96
7	102.1 ± 0.5	31.5 ± 0.14	91	3.5	1.3	0.49	0.98
8	66.6 ± 0.3	36.1 ± 0.00	100	18.9	0.0	0.93	0.99
9	80.2 ± 0.2	24.8 ± 0.04	100	1.5	3.8	0.71	0.99
10	49.9 ± 0.1	20.4 ± 0.33	75	2.5	14.1	0.57	0.97
11	139.3 ± 0.3	28.3 ± 0.04	73	9.0	0.0	0.57	0.97
12	66.9 ± 0.3	33.9 ± 0.00	100	16.9	0.0	0.93	0.98
13	60.2 ± 0.4	19.0 ± 0.20	89	3.2	5.8	0.81	0.98
14	76.3 ± 0.2	22.7 ± 0.03	83	7.0	6.0	0.86	0.93
15	36.8 ± 0.0	11.4 ± 0.00	100	8.8	3.9	0.88	0.00
16	101.2 ± 0.8	33.6 ± 0.00	100	12.7	0.0	0.94	0.99
17	94.4 ± 0.8	32.6 ± 0.00	100	21.4	0.0	0.83	0.96
18	27.5 ± 0.0	9.1 ± 0.00	100	6.9	0.0	0.55	0.96
mean±sd			93.2±11.1	9.7±6.5	5.4±10.6	0.78±0.16	0.92±0.23

C_{max} : Estimated maximum compliance; $P_{plat}(C_{max})$: Plateau pressure at which maximum compliance was estimated; *trend*: Percentage of correctly predicted position of $P_{plat}(C_{max})$; ΔC_{max} , $\Delta P_{plat}(C_{max})$: Percentage difference of predicted and originally measured value; CC_{GP} , CC_{M5P} : Correlation coefficient of model generated by GP, M5P respectively.

Table 3. Results for experimental setting (2): Training data sets were built by alternately leaving out one patient data set. The left out data set was used for testing.

<i>Patient</i>	C_{max} ml/mbar mean±sd	$P_{plat}(C_{max})$ mbar mean±sd	<i>trend</i> %	ΔC_{max} %	$\Delta P_{plat}(C_{max})$ %	CC_{GP}	CC_{M5P}
1	48.9 ± 5.0	31.5 ± 0.2	0	37.5	28.6	0.02	0.50
2	92.8 ± 5.0	34.7 ± 2.8	90	23.6	22.2	0.47	0.41
3	73.0 ± 17.1	29.8 ± 2.9	80	1.7	1.8	0.23	0.19
4	98.7 ± 17.8	27.1 ± 1.7	60	30.2	26.4	0.25	0.24
5	40.8 ± 2.8	9.7 ± 11.6	67	46.2	18.8	0.32	-0.29
6	46.2 ± 2.8	26.7 ± 2.9	44	22.4	27.8	0.55	-0.12
7	105.6 ± 11.2	33.9 ± 2.2	91	0.1	6.9	0.34	0.16
8	59.3 ± 5.8	31.2 ± 1.3	63	27.9	13.7	0.52	0.32
9	99.5 ± 9.5	2.8 ± 1.4	55	22.2	37.7	0.40	0.29
10	66.7 ± 5.1	33.3 ± 6.8	56	30.3	40.5	-0.04	-0.14
11	83.5 ± 5.4	32.2 ± 1.9	67	45.4	19.7	0.28	0.33
12	60.8 ± 5.3	33.7 ± 0.6	100	24.4	0.6	0.63	0.22
13	60.5 ± 7.3	8.1 ± 2.3	56	2.7	39.8	0.04	-0.07
14	99.8 ± 20.1	38.3 ± 4.5	67	21.7	78.8	0.52	0.06
15	70.5 ± 0.0	17.7 ± 0.0	100	74.8	61.0	0.35	0.35
16	92.7 ± 8.6	3.4 ± 0.4	100	20.0	0.4	0.60	0.43
17	79.5 ± 3.0	32.6 ± 0.0	100	33.8	0.0	0.78	0.36
18	74.5 ± 12.0	37.1 ± 3.4	0	152.1	308.4	-0.09	0.07
mean±sd			66.3±30.3	34.3±34.3	40.7±70.1	0.34±0.24	0.18±0.22

C_{max} : Estimated maximum compliance; $P_{plat}(C_{max})$: Plateau pressure at which maximum compliance was estimated; *trend*: Percentage of correctly predicted position of $P_{plat}(C_{max})$; ΔC_{max} , $\Delta P_{plat}(C_{max})$: Percentage difference of predicted and originally measured value; CC_{GP} , CC_{M5P} : Correlation coefficient of model generated by GP, M5P respectively.